EasyChair Preprint

№ 5175

Evaluation of Cu-Al-Be SMA Wear Behaviour using Taguchi Approach

P Rajendra, Pradeep K V Kumar, K R Phaneesh and Madeva Nagaral

March 18, 2021

Evaluation of Cu-Al-Be SMA wear behaviour using Taguchi Approach

Rajendra P[1], Pradeep Kumar K V[2*], Dr. K R Phaneesh[3], Dr. Madeva Nagaral[4]

[1,2,3] Department of Mechanical Engineering, Ramaiah Institute of Technology, Bengaluru 560054
*pradeepkv@msrit.edu

[4]Aircraft Research and Design Centre, Hindustan Aeronautics Limited, Bengaluru 560037

Abstract:

The preparation of Cu-Al-Be SMAs is the focus of this experimental work. The goal was to economically prepare them using Gravity die casting and an induction furnace. Martensitic phase was obtained by subjecting the casts to suitable thermal procedure. Shape memory effect and Hardness were evaluated for verification using Bend test and Vickers hardness equipment respectively. It was observed that with an increase in small addition of Be increases the hardness of alloy. After confirmation of SME, the wear test of Cu-Al-Be SMA's was performed using Pin on disc equipment. The three discrete parameters namely "sliding speed", "applied load" and "sliding distance" were analyzed using Taguchi technique. The experiment plan is generated by Taguchi's technique and based on "L27 orthogonal array" the experiments were conducted. The optimal wear properties under the impact of three discrete parameters were found using ANOVA and regression equations developed. This showed that with rising sliding distance and load, wear loss rises, while with rising sliding speed, it reduces. Based on the "smaller the best" principle, dry sliding wear resistance was evaluated and validation was performed to validate the experimental findings. SEM is used to study the morphology of worn surface and its wear mechanisms. Microstructural studies showed that adhesive, abrasive, brinelling and surface fatigue wear mechanisms are major contributors to this SMA alloy wear.

Keywords: Shape Memory Alloys, Wear Mechanisms, Taguchi Approach, Signal to Noise Ratio, Surface Fatigue

1 Introduction

SMAs are a category of metallic materials exhibiting the potential to revert to any previously defined shape or scale when exposed to the required thermal procedure. Generally, these materials will be deformed plastically at any relatively low temperature, and before the deformation, they can revert to their shape following exposure to some higher temperature [1]. Materials that only show shape memory when heated are recognized as possessing a one-way shape memory. On re-cooling, certain materials often experience a shift in shape. These materials provide a memory of the two-way form. While the shape memory effect is known to manifest a comparatively large range of alloys, only those that can regain significant quantities of strain or that produce significant force upon changing shape are of commercial concern. Nickel-titanium alloys and copper-base alloys such as Cu-Zn-Al and Cu-Al-Ni are some shape memory alloys. [2].

A shape memory alloy produces thermos-elastic martensite and undergoes a martensitic transformation that enables the alloy to deform below the transformation temperature through a

twinning process. When the twin configuration returns to the parent phase after heating, the deformation is then reversed. [3].

SMA's wear behavior is related to the martensitic thermo-elastic transformation. Until undergoing plastic deformation and subsequent cracks triggered through wear, these alloys can consume a significant amount of energy due to this transformation. In this study, the influence of "sliding speed" and "applied load" on the dry wear action of Cu-Zn-Al alloys was identified. For the various alloys, weight loss was studied as a result of the Ms transition temperature at various “sliding speeds” and “applied loads” [4]. As a function of load, the weight loss and friction coefficient of the alloys displayed linear and exponential relationships respectively. As a function of the sliding speed applied, the “weight loss” and “friction coefficient” of the alloys regardless on whatever stage was evident but an exponential relationship and no direct relationship was seen, respectively [5].

2 Taguchi Method

The objective here is to select the optimal levels for the parameters of its controllable device in such a way that the product is functional and exhibits a high performance level under a wide range of conditions and is also resilient against variability causing noise factors [6]. Noise factors are those that are not controllable or too costly to control. The parameters that can be set and retained are control factors (design features). While designing the experiment, the choice of parameters and levels is an essential step. For a different teast, parameters and levels can differ to study the wear behavior of Cu-Al-Be SMA by using the pin on disc machine; these are factors that affect the performance response (wear). [7]

Table 1: Control Factors and Levels

Factor	**Unit**	**Level1**	**Level2**	**Level3**
Sliding speed	rpm	40	80	120
Applied Load	N	5	10	15
Sliding distance	m	500	1000	1500
Material	Wt.%	CAB1	CAB2	CAB3

The choice of a suitable Orthogonal Array (OA) depends on the overall degree of freedom of the parameters of the procedure. DOF are characterized as the number of process parameter comparisons that are made to decide which degree is better and how much better it is specifically. Therefore, in this case, each parameter has three levels to analyze the wear characteristic by using the pin on the disc machine; the overall DOF for the parameters is equal to 27.

3 Experimental Setup

As per ASTM G99-95 standards, a pin-on-disc mechanical assembly shown in Fig 1 is utilized to explore the dry sliding wear properties of selected material. The wear samples were cut from as-cast samples of Diameter-8mm and height-30mm and subjected to thermo-mechanical treatment, then metallographically machined and polished. In Figure 2, the Dry-sliding wear test flow chart is shown. A standard electronic measuring unit having an LC of 1/10000 gm was used to record the specimen weights.

During the test, the pin was pressed against the counterpart that rotated against the EN31 steel disk with a hardness of 60 HRc by applying the load, as per the Taguchi table. The specimens were taken out, rinsed with propanone, dried, measured after running over a set sliding distance to assess weight reduction by wearing. The weight variation determined pre and post-test shows dry sliding wear of the sample's selected as well as volume loss estimated. As a function of the "sliding speed", "applied load", and the "sliding distance", the wear behaviour of the selected material was studied [8].

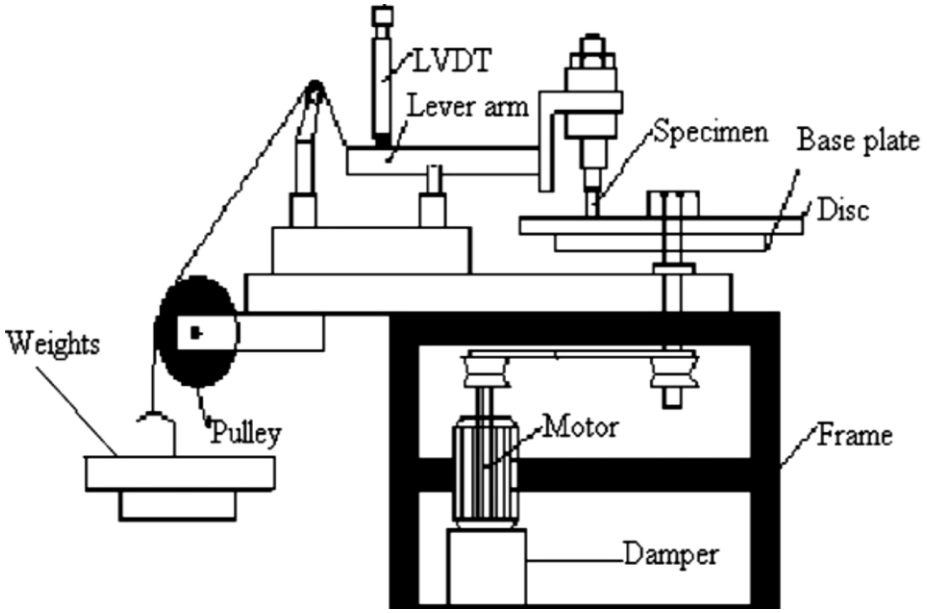

Figure 1: Pin-on-disc Mechanical Assembly [7].

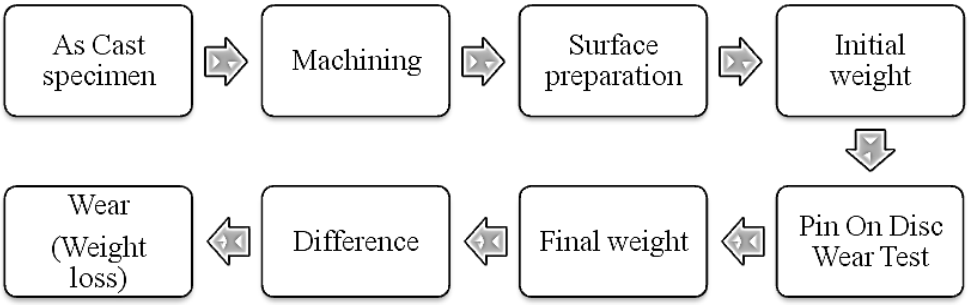

Figure 2: Dry-sliding wear test flow chart

4. RESULTS AND DISCUSSION

4.1 Alloy Composition

In an induction furnace, Cu-Al-Be SMAs with a nominal composition given in Table 2 were prepared. The production procedure and thermomechanical processing of the alloys to obtain strips with a final thickness of 1 mm and cylindrical specimen used for wear test having 8mmx 30mm (Diameter x Height) as per ASTM Standard.

Table 2: Chemical composition of the Cu-Al-Be SMA's

Alloy ID	Chemical Composition, wt%		
	Cu	Al	Be
CAB1	88.38	11.20	0.42
CAB2	88.05	11.50	0.45
CAB3	87.83	11.70	0.47

4.2 Microstructural Studies

Using a low-speed diamond saw, samples were cut. They were mechanically polished to achieve a very fine polished surface in emery sheets of 200-2000 grid scale, followed by cloth polishing with 0.1 mm alumina paste. Samples were etched into 2g K2 Cr2 O7 - 8ml H2SO4 - 2ml HCl - 100ml H2O etchant solution. These samples were studied at 50X magnification under an upright optical microscope (Olympus-Japan).

Figure 3: Optical Microscope

The crystallographic analysis showed that there are very definite crystal orientations of the martensite plates given the original structure. Martensitic transformation also leaves characteristic surface markings. The surface contrast due to a partial martensitic transformation in an alloy is seen from figure 4 to 6. The dark bands are remnants of martensite plates that have extended and collide with the surface that leads to a surface upheaval across the sample volume. Next, the long ones emerged, and shorter ones appeared between them, the creation of which was impeded by the long ones.

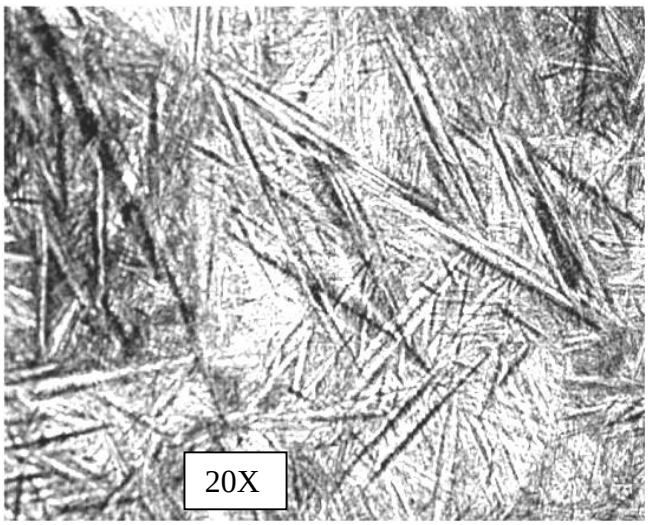

Figure 4: Martensite observed for the composition CAB1

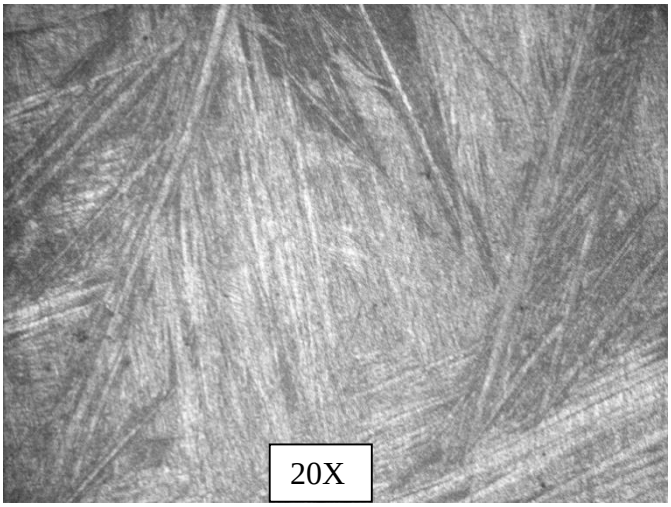

Figure 5: Martensite observed for the composition CAB2

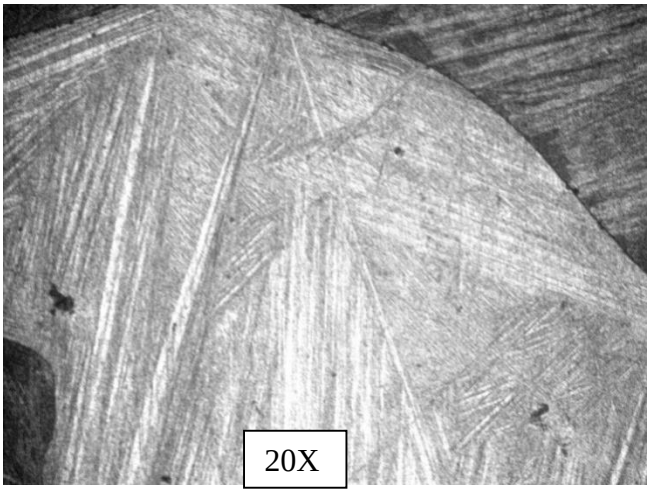

Figure 6: Martensite observed for the composition CAB3

4.3 Taguchi Results

Table 3: Orthogonal arrays (L27) Of Taguchi for wear test and S/N ratios of Cu-Al-Be SMA

Exp. No.	Sliding speed, S(rpm)	Load, L (N)	Sliding distance, D (m)	Material, CAB (Wt %)	Weight loss, WL (gm)	SNRA
1	40	5	500	CAB1	0.0020	53.9794
2	40	5	1000	CAB2	0.0045	46.9357
3	40	5	1500	CAB3	0.0065	43.7417
4	40	10	500	CAB2	0.0045	46.9357
5	40	10	1000	CAB3	0.0074	42.6154
6	40	10	1500	CAB1	0.0111	39.0935
7	40	15	500	CAB3	0.0043	47.3306
8	40	15	1000	CAB1	0.0104	39.6593
9	40	15	1500	CAB2	0.0136	37.4573
10	80	5	500	CAB2	0.0007	63.098
11	80	5	1000	CAB3	0.0035	49.1186
12	80	5	1500	CAB1	0.0064	43.8764
13	80	10	500	CAB3	0.0020	53.9794
14	80	10	1000	CAB1	0.0052	45.6799
15	80	10	1500	CAB2	0.0072	42.8534
16	80	15	500	CAB1	0.0037	48.636
17	80	15	1000	CAB2	0.0078	42.1581
18	80	15	1500	CAB3	0.0098	40.1755
19	120	5	500	CAB3	0.0005	66.0206
20	120	5	1000	CAB1	0.0032	49.897
21	120	5	1500	CAB2	0.0076	42.3837
22	120	10	500	CAB1	0.0045	46.9357
23	120	10	1000	CAB2	0.0058	44.6658
24	120	10	1500	CAB3	0.0099	40.0654
25	120	15	500	CAB2	0.0030	50.4576
26	120	15	1000	CAB3	0.0060	44.437
27	120	15	1500	CAB1	0.0141	37.0156

Table 4: Optimal process parameter level for wear in Cu-Al-Be SMA

Exp. No.	Sliding speed, S(rpm)	Load, L (N)	Sliding distance, D (m)	Weight loss, WL (gm)	SNRA
9	40	15	1500	0.013620	37.4573

The model's aim is to reduce wear loss. S/N-ratio tests the exposure to non-controlled external influencing factors (noise factors) of the quality feature monitored in a standardized manner.

The experiment attempts to determine S/N-ratio for the outcome (wear loss). It focuses on type of character being evaluated, encapsulating multiple data-points in a trial. It is possible to classify the Signal to Noise ratio features into 3 groups, viz. "nominal is the best", "larger the better" & "smaller the better".

The "smaller the better" feature was opted in this study to examine Cu-Al-Be SMAs dry-sliding wear behavior. S/N-ratio for 3 factors and 3 variables are calculated by smaller-is-better characteristics selected as we attempt to minimize wear loss.

“Smaller the better” feature:

Signal to Noise Ratio = $-10\log(1/n)\ (\Sigma y^2)$

Where n = No. of trials.

y = trial data.

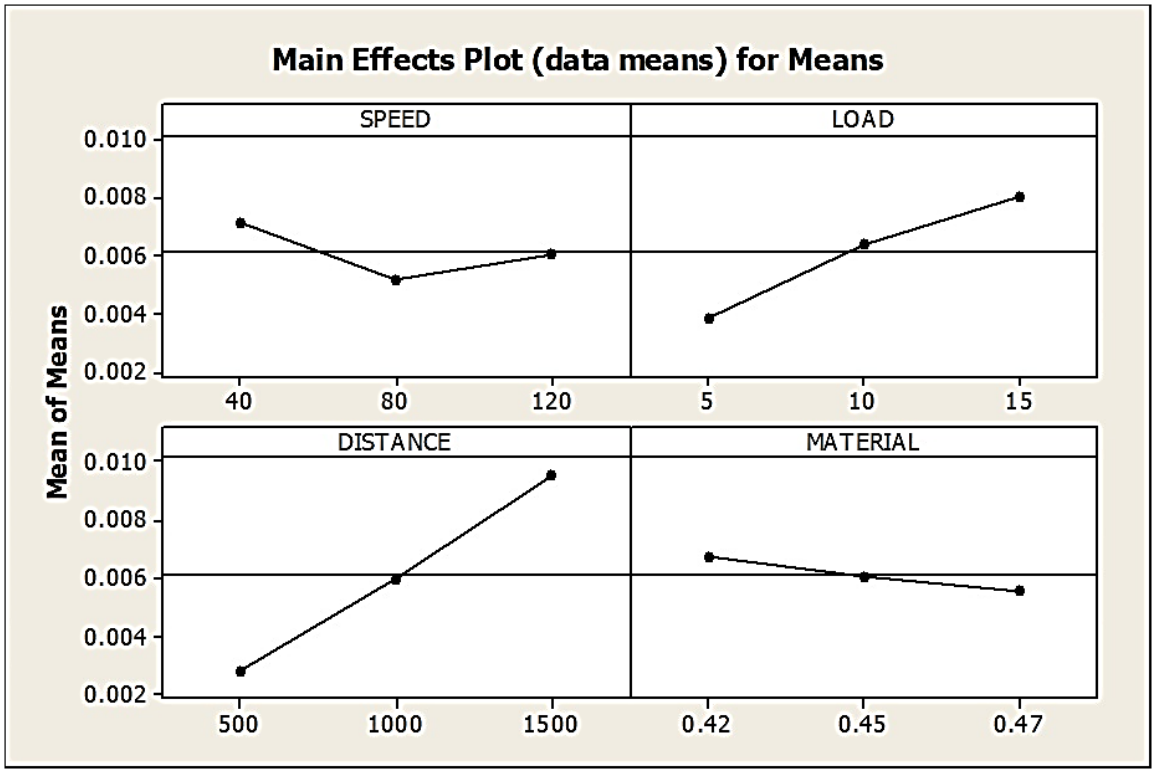

Fig 7: Main effects plot for means - Weight loss

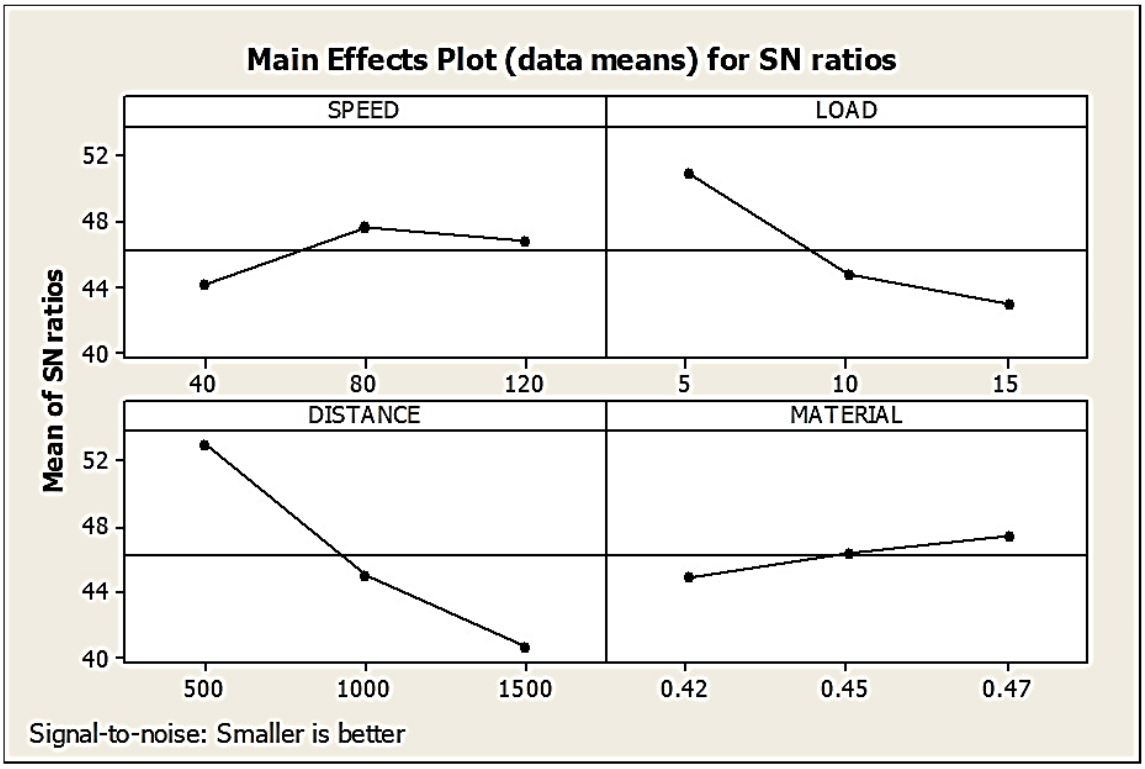

Fig 8: Main effects plot for S/N Ratios - Weight loss

The optimal conditions resulting in weight loss are seen in Figures 7 and 8 based on the interpretation of these experimental findings with the aid of signal to noise ratio. The statistics show that the first sliding velocity level, the third load level, the third sliding distance level and the first material level in weight percent are the optimal results in Table 5.

Table 5: ANOVA for wear of Cu-Al-Be SMA

Factor	Sum of squares	Degree of freedom	Variance	F – value	Test F	% of contribution
Sliding distance	2.07	2	1.035	34.5	8.65[a]	60.44
Load	0.84	2	0.42	14	8.65[a]	24.26
Sliding speed	0.19	2	0.095	3.2	3.11[c]	5.15
S*D	0.005	4	0.0125	0.83	-	0.59
S*L	0.09	4	0.0225	1.5	-	-
L*D	0.1	4	0.025	1.66	-	-
Error	0.06	8	0.0075			13.04
Total	3.4	26				100

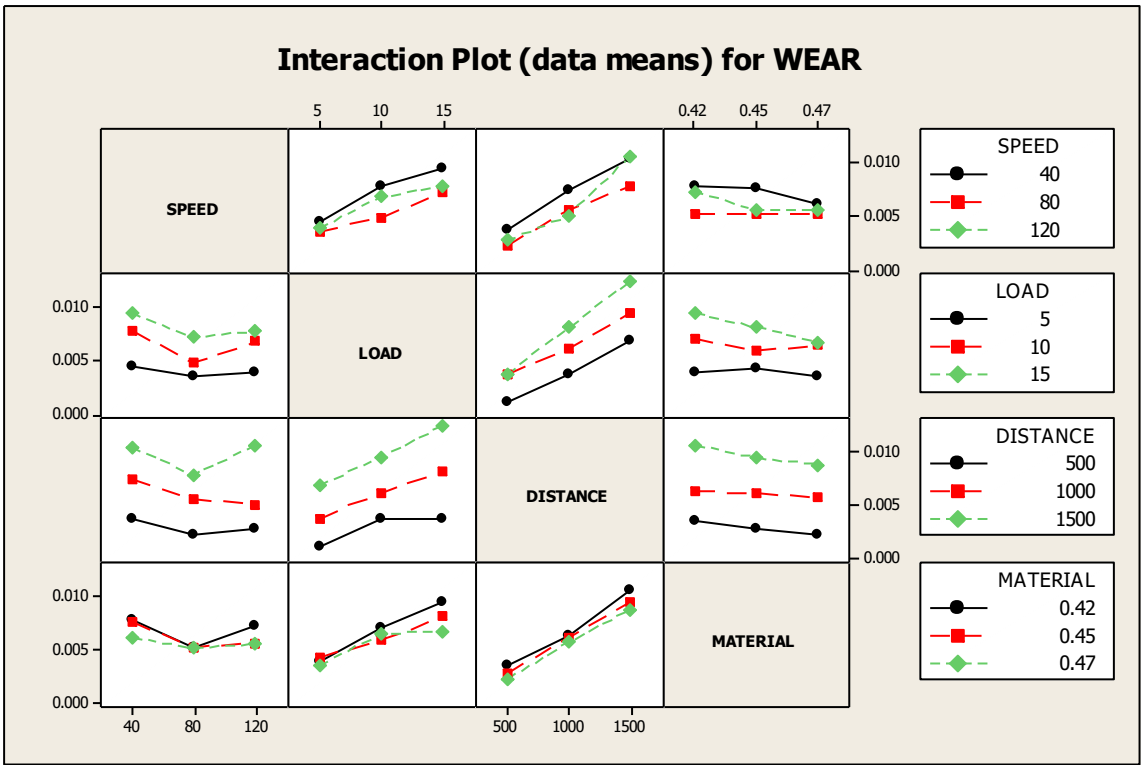

Fig 9: Interaction plot for Weight loss

The test outcomes were examined using ANOVA used to explore impact of wear variables specifically: sliding speed, load & sliding distance. These variables majorly affect the SMA performance. By conducting ANOVA [9] its very well may chose autonomous variable prevails on another & rate commitment with specific free variable.

The "sliding distance" can be found to have the greater impact (Pr = 60.44 %) on weight loss for Cu-Al-Be Shape Memory Alloys from Table 5. Therefore, sliding time, accompanied by applied loads, is a significant control factor considered during the wear process (P = 24.26 %) and sliding velocity (Pr = 5.15 %). The terms of interaction have little to no impact on weight loss & just 13.04 % of the pooled errors. It is concluded from the variance & Signal to Noise ratio study that the sliding distance, followed by load & sliding speed, has the highest contribution to weight loss.

4.4 Multiple Linear Regression Models

The MLR analysis attempts to model and to obtain the connection between at least two indicator factors and reaction factors by fitting a direct condition to the noticed information. To evaluate the relationship of wear parameters: “sliding distance”, “applied load”, “sliding speed” & material. Using statistical program "MINITAB R14", the “dry sliding wear”, “weight loss” and “wear MLR models” were obtained with statistically relevant terms included in the model.

Model's regression coefficient given by

$$\mathbf{WEAR\ (_{CAB\ SMA})} = (0.00678) - (0.000013 * S) + (0.000418 * L) + (0.000007 * D) - (0.0236 * M)$$

Where W = Weight loss (gm)

S = Sliding Speed (rpm)

L = Applied Load (N)

D = Sliding Distance (m)
M = Material in (wt %)
R - Sq = 88.5%

4.5 Experiment of Conformation

The analytical and practical results are contrasted with the aid of the confirmation test, which can be performed with the program "MINITAB-14". Comparison of wear results from the mathematical model can be compared with the various values obtained experimentally. The Multiple linear regression equation derived and correlates the evaluation of the selected material with a reasonable degree of approximation.

Table 6: Factors and Levels assignment for the conformation Experiment

Factor	**Units**	**Level1**	**Level2**	**Level3**
Sliding speed	rpm	50	75	100
Load	N	8	12	16
Sliding distance	M	600	900	1200
Material	Wt%	CAB1	CAB2	CAB3

Table 7: The output of the conformation experiment and the Regression Model comparison

Exp. No.	**Exp. weight loss (gm)**	**Regression model (7), weight loss (gm)**	**% Error**
1	0.003892	0.003762	3.4
2	0.006578	0.006501	1.179
3	0.010134	0.009476	6.89

From the investigation, Actual weight reduction is discovered to be fluctuating from the determined one utilizing the regression equation, and for weight reduction, the blunder rate varies between 1.179 to 6.89 percent. These qualities intently taking after the real information with least blunder, investigations by the Taguchi approach found effective for computing weight reduction from regression equation. These values exactly represent the real data with minimal error.

4.6 Morphology of worn surface (SEM images)

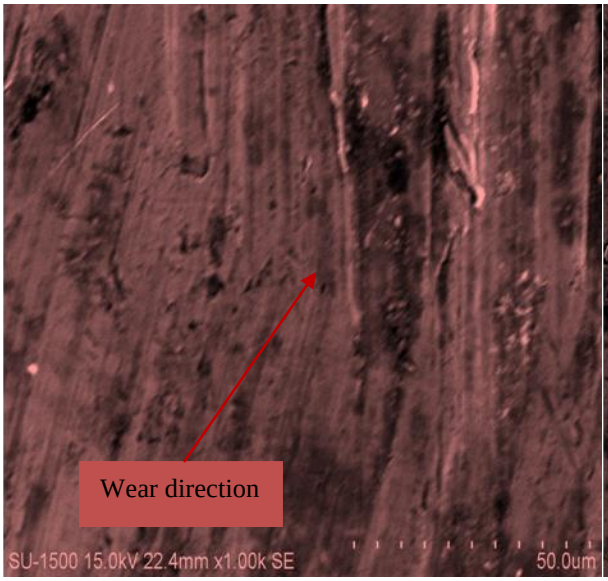

Fig 4.10: (a) Wear direction

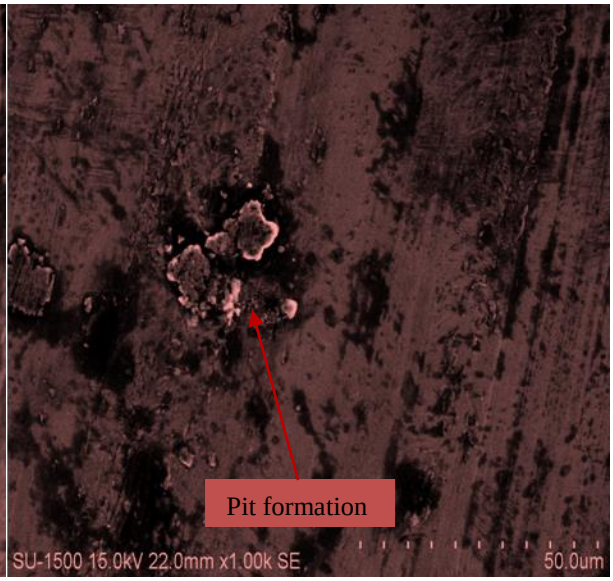

Fig 4.10: (b) Pit formation

Fig 4.10: (a) illustrate that the path of wear exists along the disk direction, and Fig 4.10: (b) It occurs because of the repetitive loading and unloading cycles, several surfaces or sub-surface cracks form and eventually lead to the breakup into huge sections, resulting in huge surface concavity.

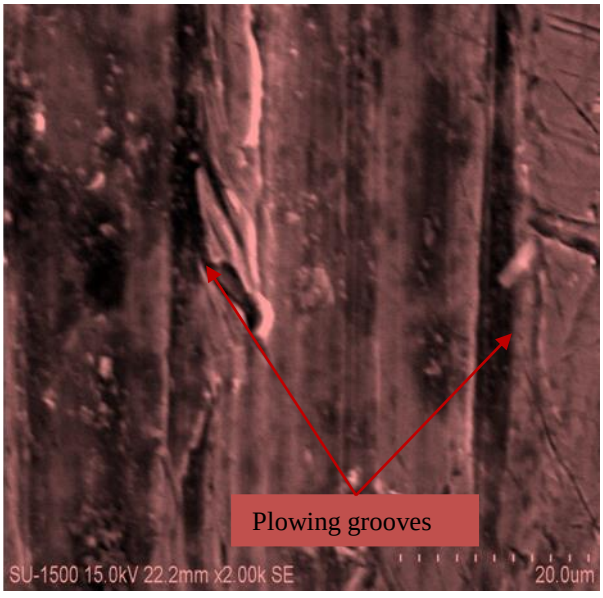

Fig 4.10: (c)Abrasive wear

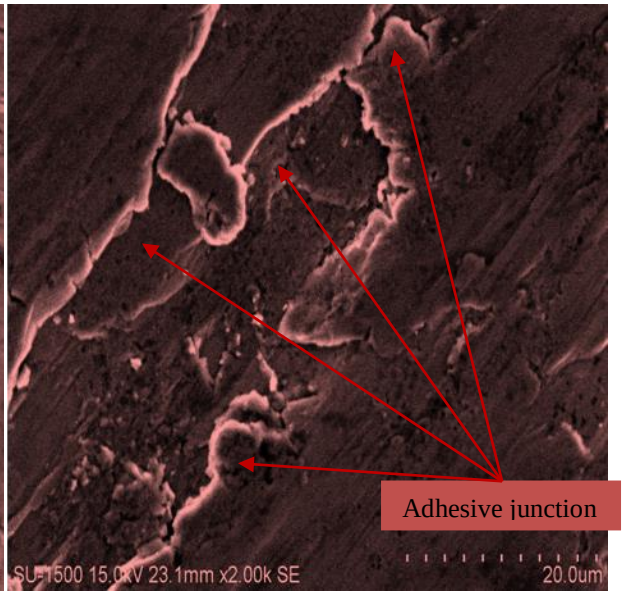

Fig 4.10: (d)Adhesive wear

Fig 4.10: (c) The abrasive wear, the plowing grooves resulting from the interaction, micro-cutting, and plastic deformation are illustrated. Many surfaces or subsurface cracks are developed owing to repetitive loading and unloading cycles and ultimately result in surface breakup.

Accumulation of adhesive junctions, abrasive deformation and wear chips, and mechanical locking of surface pits can be due to the crests that look like pearls in Fig 4.10: (d). During the sliding wear process, these pearl-like crests can increase the fluctuation of the friction coefficient and quickly increase the loss of weight due to mechanical fracture.

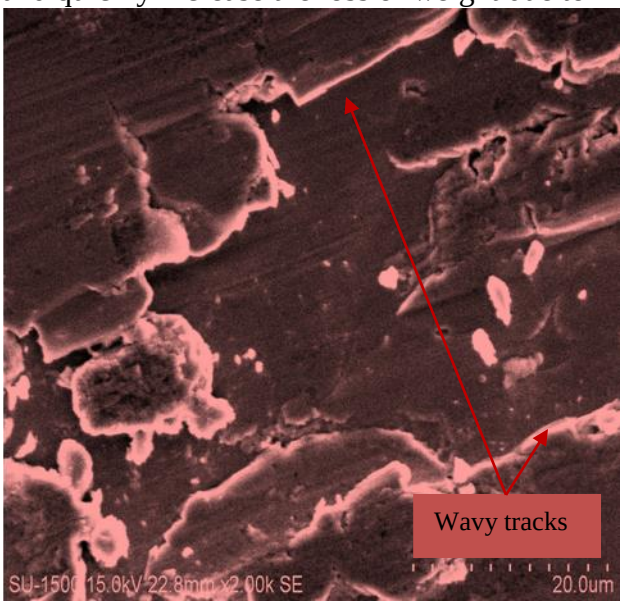

Fig 4.10: (e) Brinelling wear

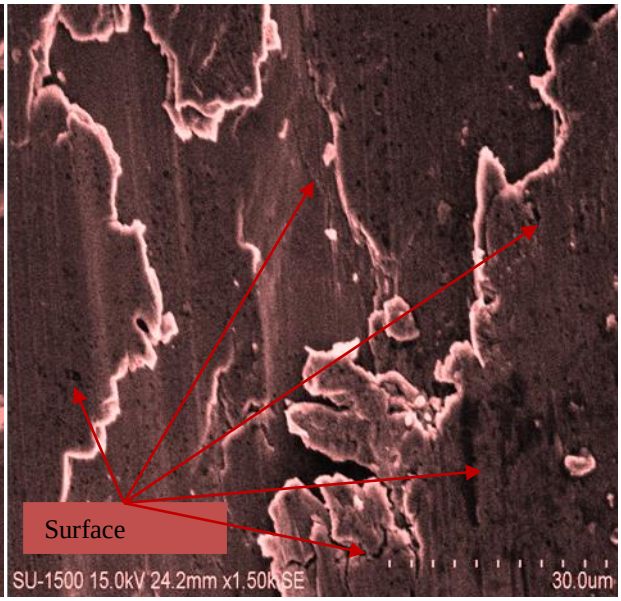

Fig 4.10: (f) Surface fatigue

Fig 4.10: (e) The wavy tracks on the outer surface are shown. Its known as “brinelling wear” that arises from the softer materials' plastic deformation. It should be realized that the brinelling wear phenomenon can increase the coefficient of friction, but it has no contribution to loss of weight. Fig 4.10: (f) Several surfaces or subsurface cracks form due to repetitive loading and unloading cycles and ultimately lead to the breakup of the surface into large fragments, leaving large pits on the surface.

5. Conclusions

Based on the experimental analysis and investigations in the present work, it can be concluded that:

1. The Taguchi optimization technique was used to design the pin on disc wear test using 3 distinct parameters namely, Sliding Distance, Applied Load and Sliding Speed.
2. Pin on disc wear test shows that the increase in sliding distance and applied load wear loss increases, but the wear loss decreases with the increase in sliding speed.
3. The optimal outcome of under-considered parameters is shown by Signal to Noise ratio graphs acquired from “Taguchi Minitab14” Application.
4. ANOVA tests also verified that the 3 distinct parameters play key role in wear.
5. The error from confirmation test varies between 1.179 to 6.89 percent, leading to the inference that DOE was effective in using the Taguchi method for measuring erosion with regression model.
6. Four main mechanisms, namely “abrasive”, “adhesive”, “brinelling wear” and “surface fatigue”, are responsible for significant contributions to the wear characteristics of the studied SMA.

References

[1] Huang, W. M., Ding, Z., Wang, C. C., Wei, J., Zhao, Y., & Purnawali, H. (2010). Shape memory materials. Materials today, 13(7-8), 54-61.

[2] Christian, J. W. (2002). The theory of transformations in metals and alloys. Newnes.

[3] Dasgupta, R. (2014). A look into Cu-based shape memory alloys: Present scenario and future prospects. Journal of Materials Research, 29(16),

[4] Ma, J., Karaman, I., & Noebe, R. D. (2010). High temperature shape memory alloys. International Materials Reviews, 55(5), 257-315 1681.

[5] Pena, J., Gil, F. J., & Guilemany, J. M. (2006). Load and sliding velocity effect in dry sliding wear behavior of CuZnAl shape memory alloys. Metallurgical and Materials Transactions A, 37(4), 1175-1181.

[6] Unal, R., & Dean, E. B. (1991). Design for cost and quality: the robust design approach. Journal of Parametrics, 11(1), 73-93.

[7] Weiss, I., & Semiatin, S. L. (1999). Thermomechanical processing of alpha titanium alloys—an overview. Materials Science and Engineering: A, 263(2), 243-256.

[8] Savadamuthu, L., Muthu, S., Rakhul, T., & Jothimani, S. (2013). Multi characteristic optimization in wire cut EDM by using taquchi data envelopment analysis based ranking methodology. International Review of Mechanical Engineering (IREME), 7(3), 468-473

[9] Piedboeuf, M. C., Gauvin, R., & Thomas, M. (1998). Damping behaviour of shape memory alloys: strain amplitude, frequency and temperature effects. Journal of Sound and Vibration, 214(5), 885-901.

[10] Mitchell, T. J., & Beauchamp, J. J. (1988). Bayesian variable selection in linear regression. Journal of the american statistical association, 83(404), 1023-1032.

[11] Pasha, B. M., Budan, D. A., Basavarajappa, S., Yadav, S. M., & Nizamuddin, B. A. (2013). Studies on wear resistance of PTFE filled with glass and bronze particles based on Taguchi technique. Journal of Thermoplastic Composite Materials, 26(2), 243-259.

[12] Marimuthu, P. and Chandrasekaran, K. (2012) 'Machinability study on stainless steel and optimum setting of cutting parameters in turning process using Taguchi design of experiments', Int. J. Materials and Product Technology, Vol. 43, Nos. 1/2/3/4,pp.122–133. http://dx.doi.org/10.1504/ijmpt.2012.047648

[13] Ghani, J.A., Choudhury, I.A. and Hasan, H.H. (2004) 'Application of Taguchi method in the optimizations of end milling operations', J. Mat. Proc. Tech., Vol. 145, No. 1, pp.84–92.

[14] Jeyapaul, R., Shahabudeen, P. and Krishnaiah, K. (2006) 'Simultaneous optimization of multi-response problems in the Taguchi method using genetic algorithm', Int. J. Adv. Manuf. Tech., Vol. 30, Nos. 9–10, pp. 870–878. http://dx.doi.org/10.1007/s00170-005-0095-9

[15] Muthukrishnan; (2008, a) Optimization of machining parameters of Al/sic – MMC with ANOVA and ANN analysis, J. Mater. Process. Tech, Vol.209, pp.225-232. http://dx.doi.org/10.1016/j.jmatprotec.2008.01.041

[16] Spuzic S, Zec M, Abhary K, Ghomashchi R and Reid I. Fractional design of experiments applied to a wear simulation. Wear 1997; 212: 131–139.

[17] Sahin Y. Wear behavior of aluminum alloy and its composites reinforced by SiC particles using statistical analysis. Mater Design 2003; 24: 95–103.

[18] Basavarajappa S, Chandramohan G and Paulo Davim J. Application of taguchi techniques to study dry sliding wear behavior of metal matrix composites. Mater Design 2007; 28: 1393–1398.

[19] Colac¸o R and Vilar R. A model for the abrasive wear of metallic matrix particle-reinforced materials. Wear 2003; 254: 625–634.
[20] Mondal DP, Das S, Jha AK and Yegnesswaran AH. Abrasive wear of Al alloy-Al2O3 particle reinforced composite: A study on the combined effect of load and size of abrasive. Wear 1998; 223: 131–138.
[21] Prasad BK, Das S, Jha AK, Modi OP, Dasgupta R and Yegneswaran AH. Factors controlling the abrasive wear response of a zinc-based alloys silicon carbide particle composite. Compos A 1997; 28: 301–308.
[22] Taguchi G and Konishi S. Taguchi methods: orthogonal arrays and linear graphs; tools for quality engineering. Dearborn, MI: American Supplier Institute Inc, 1987.
[23] Phillip J Ross. Taguchi techniques for quality engineering 2nd ed. New York: Tata McGraw-Hill Edition, 2005.
[24] Roy KR. A primer on taguchi method. New York: Van Nostrad reinhold, 1990.
[25] U. Sarı and T. Kirindi Effects of deformation on microstructure and mechanical properties of a Cu-Al-Ni shape memory alloy. Mater. Charact. 59, 920 (2008).
[26] M. Miki, N. Maeshiro and Y. Ogino Effects of additional elements on the super plasticity of a Cu-14Al-3Ni shape memory alloy. Mater. Trans., JIM 30(12), 999 (1989).
[27] N. Shajil, D. Das, and L. Chandrasekaran: Effects of cycling on the pseudoelastic properties of CuAlMnNi & TiNi based pseudoelastic alloys. Int. J. Struct. Changes Solids – Mech. Appl. 1(1), 171 (2009).
[28] Y. Chen, X. Zhang, D.C. Dunand, and C.A. Schuh: Shape memory and superelasticity in polycrystalline Cu–Al–Ni microwires. Appl. Phys. Lett. 95(17), 906 (2009).
[29] Y. Sutou, N. Koeda, T. Omori, R. Kainuma, and K. Ishida: Effects of ageing on bainitic and thermally induced martensitic transformations in ductile Cu–Al–Mn-based shape memory alloys. Acta Mater. 57, 5748 (2009).
[30] Y. Sutou, N. Koeda, T. Omori, R. Kainuma, and K. Ishida: Effect of aging on stress induced martensitic transformations in ductile Cu-Al-Mn based shape memory alloys. Acta Mater. 57, 5759 (2009).
[31] S. K. Vajpai, R. K. Dube and S. Sangal: Processing and characterization of Cu-Al-Ni shape memory alloy strips prepared from pre alloyed powder by hot densification rolling of powder preforms. Metall. Mater. Trans. 42A, 3178 (2011).
[32] R. Zengin and M. Ceylan: The effects of neutron irradiation on oxidation behavior, microstructure and transformation temperatures of Cu–12.7 wt.% Al–5 wt.% Ni–2 wt.% Mn shape memory alloy. Mater. Lett. 58, 55 (2003).
[33] R. Zengin: Microstructure and oxidation properties of a neutron irradiated Cu–13.5wt% Al–4 wt% Ni shape memory alloy. Phys. B 363, 110 (2005).
[34] S. Stanciu, L-G. Bujoreanu, B. Özkal, M. Lutfi Öveçoğlu, and A.V. Sandu: Study of precipitate formation in Cu–Al–Ni–Mn–Fe shape memory alloys. J. Optoelectron. Adv. Mater.10(6),1365(2008).
[35] C. Xiaomin, H. Feng, L. Ni, and W. Xingwen: Microstructure and shape memory effect of Cu-26.1Zn-4.8Al alloy. J. Wuhan Univ. Technol., Mater. Sci. Ed. 23, 717 (2008).
[36] V. Asanovic and K. Delujc: The mechanical behavior and shape memory recovery of Cu-Zn-Al alloys. Metalurgija 13(1), 59(2007).
[37] Y. J. Bai, G. L. Geng, X. F. Bian, D. S. Sun, and S. R. Wang Influence of initial heating temperature on the reverse martensitic transformation of Cu–Zn–Al–Mn–Ni alloy. Mater. Sci. Eng., A 284, 25 (2000).

[38] N. Kayali, S. Ozgen, and O. Adigiizel: The influence of ageing on martensite morphology in shape memory Cu–Zn–Al alloys. J. Phys. IV France 7(C5), 317 (1997).
[39] V.H.C. de Albuquerque, T.A. de A. Melo, R.M. Gomes, S.J.G. de Limaa, and J.M.R.S. Tavares: Grain size and temperature influence on the toughness of a Cu-Al-Be shape memory alloy. Mater. Sci. Eng., A 528, 459 (2010).
[40] P. Zhang, A. Ma, S. Lu, P. Lin, J. Jiang, H. Ma, and C. Chu: Effect of equal channel angular pressing and heat treatment on the microstructure of Cu-Al-Be-B shape memory alloy. Mater. Lett. 63, 2676 (2009).
[41] S. Montecinos and A. Cuniberti: Martensitic transformation and grain size in a Cu-Al-Be alloy. Procedia Mater. Sci. 1, 149 (2012).
[42] A. Abu Arab and M. Ahlers: The stabilization of martensite in Cu-Zn-Al alloys. Acta Metall. 36(9), 2627 (1988).
[43] F. Saule and M. Ahlers: Stability, stabilization and lattice parameters in Cu-Zn-Al martensites. Acta Metall. Mater. 43(6), 2373 (1995).
[44] N. Kuwano, T. Doi, and T. Eguchi Annealing behavior of heavily deformed martensites of Cu-Al alloys. Mater. Trans., JIM 20, 37 (1979).
[45] S. Sathish, U.S. Mallik, and T. N. Raju: Microstructure and shape memory effect of Cu-Zn-Ni shape memory alloys. J. Miner. Mater. Charact. Eng. 2, 71 (2014).
[46] S. Pourkhorshidi, N. Parvin, M.S. Kenevisi, M. Naeimi, and H. Ebrahimnia Khaniki: A study on the microstructure and properties of Cu-based shape memory alloy produced by hot extrusion of mechanically alloyed powders. Mater. Sci. Eng., A 556, 658 (2012).
[47] J. M. Guilemany, F. Peregrín, F. C. Lovey, N. LLorca and E. Cesari TEM study of band martensite in Cu-Al-Mn shape memory alloys. Mater. Charact. 26, 23 (1991).
[48] E. Hornbogen, V. Mertinger, and J. Spielfield: Ausageing and ausforming of a copper based shape memory alloy with high transformation temperatures. Z. Metallkd. 90(5), 318 (1999).
[49] O. Adigiizel: Martensite ordering and stabilization in copper based shape memory alloys. Mater. Res. Bull. 30(6), 755 (1995).
[50] S.N. Sauda, E. Hamzaha, T. Abubakara, and R. Hosseinian: A review on influence of alloying elements on the microstructure and mechanical properties of Cu-Al-Ni shape memory alloys. Jurnal Reknologi (Sciences & Engineering) 64(1), 51 (2013).
[51] H. Sakamoto, Y. Kijima, and K. Shimizu: Fatigue and fracture characteristics of polycrystalline Cu-Al-Ni shape memory alloys. Mater. Trans., JIM 23, 585 (1982).
[52] S. Kustov, S. Golyandin, K. Sapozhnikov, E. Cesari, J. Van Humbeeck, and R. De Batist: Influence of martensitic stabilization on the low temperature non-linear anelasticity in Cu-Zn-Al shape memory alloys. Acta Mater. 50, 3023 (2002).
[53] Y. Suotou, T. Omori, R. Kainuma and K. Ishida Ductile Cu-Al-Mn based shape memory alloys: General properties and applications. Mater. Sci. Technol. 24(8), 896 (2008).
[54] U.S. Mallik and V. Sampath: Effect of alloying on microstructure and shape memory characteristics of Cu–Al–Mn shape memory alloys. Mater. Sci. Eng., A 481–482, 680 (2008).
[55] C. Segui, E. Cesari, and J. Van Humbeeck: Irreversibility in two stage martensitic transformation of Cu-Al-Ni and Cu-Zn-Mn alloys. Mater. Trans., JIM 31(5), 375 (1990).
[56] M. Sharma, S.K. Vajpai, and R.K. Dube: Processing and characterization of Cu-Al-Ni shape memory alloy strips prepared from elemental powders via a novel powder metallurgy route. Metall. Mater. Trans. A 41A, 2905 (2010).

[57] Z. Li, Z.Y. Pan, N. Tang, Y.B. Jiang, N. Liu, M. Fang, and F. Zheng: Cu–Al–Ni–Mn shape memory alloy processed by mechanical alloying and powder metallurgy. Mater. Sci. Eng., A 417, 225 (2006).
[58] S. Yang, Y. Su, C. Wang and X. Liu Microstructure and properties of Cu–Al–Fe high-temperature shape memory alloys. Mater. Sci. Eng., B 185, 67 (2014).
[59] Z. Xiao, M. Fang, Z. Li, T. Xiao and Q. Lei Structure and properties of ductile Cu-Al-Mn shape memory alloy synthesized by mechanical alloying and powder metallurgy. Mater. Des. 58, 451 (2014). 56. H. Funakubo: Shape Memory Alloys, 1st ed.; Gordon and Breach Science Publishers: New York, 1987; p. 226.
[60] C. M. Waymanand and T. W. Duerig An introduction to martensite and shape memory. Engineering Aspects of Shape Memory Alloys, 1st ed.; Butterworth-Heinemann: Oxford, 1990; p. 3.
[61] J. San Juan, M.L. No, and C.A. Schuh: Thermomechanical behavior at the nanoscale and size effects in shape memory alloys. J. Mater. Res. 26(19), 2461 (2011).
[62] S. Casciati: Experimental studies on the fatigue life of shape memory alloy bars. Smart Struct. Syst. 6(1), 73 (2010).
[63] J. Ortín and A. Planes: Thermodynamics of thermoelastic martensitic transformations. Acta Metall. 37(5), 1433 (1989).
[64] C.M. Wayman: Thermoelastic martensitic transformations and the shape memory effect. In Proc. of the Int. Conf. on phase Trans. In Soliak, Maleme-Chania, North-Holland, New York, 1984, p. 657.
[65] J. Van Humbeeck: High temperature shape memory alloys. Trans. ASME 12, 98 (1999).
[66] K. Marukawa and K. Tsuchiya: Two important aging effects on the martensite phase in CuZnAI alloys: Rubber effect and stabilization of martensite. J. Phys. 11, 8 (2001).
[67] D. Junkai, D. Xiangdong, L. Turab, S. Tetsuro, O. Kazuhiro, S. Jun, A. Saxena and R. Xiaobing: Microscopic mechanism of martensitic stabilization in shape-memory alloys: Atomic-level processes. Phys. Rev. B 81(22), 1 (2010).
[68] R. Romero and M. Stipcich: The stabilization of martensite in Cu-Zn-Al-Ti-B shape memory alloys. Fifth European symposium on martensitic transformations and shape memory alloys. J. Phys. 11(8), 135 (2001).
[69] Y. Sutou, T. Omoria, J.J. Wang, R. Kainuma, and K. Ishida: Characteristics of Cu–Al–Mn-based shape memory alloys and their applications. Mater. Sci. Eng., A 378, 278 (2004).